Approaching Near-Capacity on a Multi-Antenna Channel using Successive Decoding and Interference Cancellation Receivers

Mathini Sellathurai, Paul Guinand, and John Lodge

Abstract: **In this paper, we address the problem of designing multirate codes for a multiple-input and multiple-output (MIMO) system by restricting the receiver to be a successive decoding and interference cancellation type, when each of the antennas is encoded independently. Furthermore, it is assumed that the receiver knows the instantaneous fading channel states but the transmitter does not have access to them. It is well known that, in theory, minimum-mean-square error (MMSE) based successive decoding of multiple access (in multi-user communications) and MIMO channels achieves the total channel capacity. However, for this scheme to perform optimally, the optimal rates of each antenna (per-antenna rates) must be known at the transmitter. We show that the optimal per-antenna rates at the transmitter can be estimated using only the statistical characteristics of the MIMO channel in time-varying Rayleigh MIMO channel environments. Based on the results, multirate codes are designed using punctured turbo codes for a horizontal coded MIMO system. Simulation results show performances within about one to two dBs of MIMO channel capacity.**

Index Terms: **Multiple-input multiple-output (MIMO), turbo codes, successive decoding, interference cancellation, per-antenna rates, multirate coding, minimum-mean-square error (MMSE).**

I. INTRODUCTION

The idea of successive decoding, which involves decoding the users sequentially in a given order, was initially proposed in the context of an information-theoretic study of scalar output Gaussian multiple access channels [1]-[3]. In this scheme, the first user is decoded by treating the interference from other users as noise. The decoded transmitted codeword of the first user is then subtracted from the received data and the second user is decoded by treating the interference from the remaining users as noise, and so on. It is well known that, in theory, MMSE based successive decoding and interference cancellation type receivers of multiple access (in multi-user communications) and multiple-input and multiple-output (MIMO) channels achieve the total Shannon channel capacity provided that for each user (antenna) optimal rates are known [4], [5]. Thus, the channel capacity can be achieved by independent encoding and successive decoding procedures using 1-dimensional channel codes.

However, for this scheme to perform optimally, the optimal rate of each antenna must be known at the transmitter. A closely related work proposing rate and power control with successive decoding receivers for MIMO systems can be found in [6] using rate and power feedback, where it is assumed that exact channel state information is known for estimating the per-antenna rate and power. The paper also showed that the capacity degradation when doing only rate allocation is very small, indicating that the power allocation is irrelevant in most cases. However, [6] does not establish a practical method for adapting the per-antenna rates. In this paper, given only the statistics of the channel and the receiver operating SNR at the transmit end, we propose a method to adapt the rates of each of the transmit antennas.

In particular, we identify that the turbo codes as a suitable candidate to achieve near-optimal performance using the proposed scheme due to its rate adaptability (by puncturing) and high BER performances. The contributions in this paper are as follows. In time-varying MIMO Rayleigh channel environments,

- we show that the per-antenna rates can be estimated using only the statistical characteristics of the MIMO channel known at the transmitter.
- we derive a simple analytical expression for a lower bound on per-antenna rates.
- we design a multi-rate coded MIMO system using punctured turbo codes and demonstrate the efficiency of the proposed scheme using simulation results. In particular, in the framework of horizontal coded MIMO communication systems, we achieve performances within 1-2 dB of MIMO channel capacity. Our capacity analyses assume that the receiver knows the instantaneous fading channel states.

II. SYSTEM MODEL

A. MIMO System Model

Consider a MIMO system that has M transmit and N receive antennas with iid Gaussian noise at each of the receive antennas. The propagation coefficients can be arranged in an $N \times M$ random matrix. We assume that the receiver knows the channel coefficient matrix perfectly. The transmitter only knows the statistics of the matrix channel. In complex baseband representation, the system can be written considering T symbol periods as follows:

$$Y(t) = H(t)A(t) + W(t), \quad t = 1, 2, \ldots, T, \qquad (1)$$

where $A \in \mathcal{C}^{M \times T}$ and the row vector $A_i \in \mathcal{C}^{1 \times T}, i = 1, 2, \ldots, M$ corresponds to the transmitted signal at the ith antenna. Similarly, $Y \in \mathcal{C}^{N \times T}$ and each row vector $Y_i \in \mathcal{C}^{1 \times T}, i = 1, 2, \ldots, N$ corresponds to the received signal for the

Manuscript received January 31, 2003.

The authors are with the Communications Research Centre, Canada Ottawa, Ontario K2H 8S2, email: {mathini.sellathurai, paul.guinand, john.lodge}@crc.ca.

Parts of this paper were presented in Information Theory Workshop, Paris, France, April 1-4, 2003.

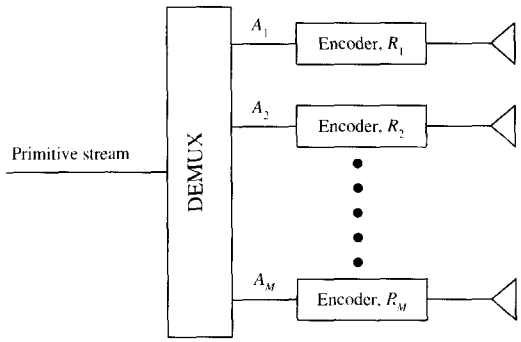

Fig. 1. Transmitter.

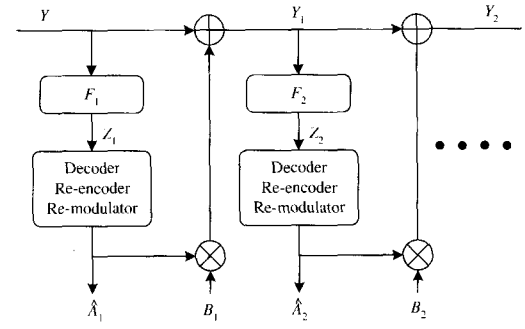

Fig. 2. Successive decoding and interference cancellation.

ith receive antenna, and $H(t) = [H_1(t), H_2(t), \ldots, H_M(t)]$, $t = 1, \ldots, T$, is the $N \times M$ channel matrix, $H_q(t) = [H_{1,q}(t), \ldots, H_{N,q}(t)]^H, 1 \leq q \leq M$, where the propagation gains from jth transmit antenna to the ith receive antenna H_{ij} are iid complex Gaussian $\mathcal{CN}(0,1)$ and the superscript $(\cdots)^H$ denotes for Hermitian transpose. The additive white noise $W \in \mathcal{C}^{N \times T}$ has iid entries $W_{ij}(t) \sim \mathcal{CN}(0, \sigma^2)$ where the the noise component has variance σ^2. We normalize the power to satisfy $E\left[\sum_{i=1}^{M} \sum_{t=1}^{T} \|A(t)\|^2\right] = PT$, where P is the total power transmitted per symbol interval.

B. Encoder-Decoder Structure

We consider a horizontal coded layered space-time structure [7] with M transmit and N receive antennas. The transmitter is illustrated in Fig. 1. In this structure, a primitive data stream is multiplexed into M substreams $A_i, i = 1, 2, \ldots, M$ and coded independently with varying code rates $R_i, i = 1, 2, \ldots, M$.

At the receiving end, the decoupling process for each of the M layers involves a combination of nulling (that is minimizing) the interference from yet undetected signals and canceling out the interference from already detected signals. Thus, the Successive Interference Cancellation receiver has two step processing: (1) Feedforward and (2) Feedback processing, which are parameterized by a set of feedforward (F) and feedback (B) filters, respectively. The function of the feedforward filters is to estimate the substreams based on the modified received signal whereas the feedback filters are used to cancel the interference from the past estimated signals as shown in Fig. 2. Without loss of generality, we assume that the substreams are decoded in the increasing order of their indexes. Therefore, in decoding the kth substream, the interference from the already past decoded substreams $1, 2, \ldots k-1$ is removed by subtracting it from the received signal to form a modified received signal which is then used to estimate the kth substream.

III. PRINCIPLE THEORETICAL RESULTS OF SUCCESSIVE DECODING

A. Successive Decoding and Interference Cancellation

Let the feedforward filters be described by the set of N-dimensional vectors $\{F_k\}_{k=1}^{M}$ and the feedback filters by the set of N-dimensional vectors $\{B_k\}_{k=1}^{M-1}$. In decoding the kth user, the interference from the already decoded antennas is removed by subtracting a linear combination of the decoded[1] streams, $\hat{A}_1, \ldots, \hat{A}_{k-1}$, and the kth antenna feedback filters from Y. Then the inner product of the resulting modified received vector (Y_{k-1}) and the kth antenna feedforward filter gives the estimation Z_k shown in Fig. 2. For the kth antenna (for the tth symbol) [3]:

$$Z_k(t) = F_k^H(t) H_k(t) A_k(t) + \sum_{j=k+1}^{M} F_k^H(t) H_j(t) A_j(t) + \sum_{j=1}^{k-1} F_k^H(t)(H_j(t) - B_j(t))\hat{A}_j(t) + F_k^H(t) W_k(t),$$

where $\hat{A}_j$ is the estimated information stream of antenna j. In RHS of the above equation, the first term is the signal of interest, the second term is the interference from the undecoded antennas, the third term is the residual interference from the previously decoded antennas and the last term corresponds to the AWGN channel. We assume that all the previous antennas are decoded error-free so that error propagation does not occur. Consequently, $\hat{A}_j$ will be replaced by A_j in the following.

B. Optimal Weights

The optimal feedforward and feedback weights that maximize the mutual information of each transmit antenna can be found by maximizing the following mutual information [3]

$$C_k = \max_{F_k, \{B_j\}_{j=1}^{k-1}} \log_2(1 + \Upsilon_k), \tag{2}$$

where Υ_k is the signal-to-interference ratio (SIR) defined by (3) as shown at the bottom of next page. To find the optimum weights, we can equally maximize the SIR, and the optimum feedback and feedforward filters are given by [3]

$$B_j = H_j, \quad 1 \leq j \leq M-1, \tag{4}$$

$$F_k = \alpha(\bar{H}_k^T \bar{H}_k + I\delta_s)^{-1} H_k, \quad 1 < k \leq M, \tag{5}$$

where $\bar{H}_i = [H_{i+1}, H_{i+2}, \ldots, H_N]$ is a $N \times (M-i)$ matrix built of the channel vectors of the $(M-i)$ interfering signals at the ith layer, $\delta_s = \frac{M}{\rho}$, $\rho = P/\sigma^2$ is the average signal-to-noise ratio per receive antenna, and $\alpha = 1 + \delta_s$. In this case, the maximum output SIR receivers are equivalent to the MMSE receivers.

[1] Interference nulling and cancellation process followed by channel decoding, re-encoding and re-modulation.

C. Per-Antenna Rates

In the following, we provide formulas for per-antenna rates subject to independent encoding at the transmitter and successive decoding at the receiver. We assume that each entry in the $N \times M$ matrix channel is a zero-mean Gaussian random variable with independent real and imaginary parts, each with variance $1/2$.

In this work, we treat the matrix channel H as ergodic so that the capacity is computed by using time averaging. For the multiple antenna channel with perfect knowledge of the fading coefficients at the receiver but not at the transmitter, the channel capacity of a system with M transmit and N receive antenna in an ergodic channel environment is given by [8]

$$C_{M,N}(\rho) = E\left[\log_2 \det\left(I_N + \frac{\rho}{M} H H^H\right)\right]. \quad (6)$$

When we restrict the decoder to be a combination of successive decoding and interference cancellation type with interference equalization based on optimal MMSE weights, the ith antenna rate is given by

$$R_{\{i,(M,N),MMSE\}}(\rho) = E[\log_2(1+\Upsilon_i)] \quad i = 1,2,\ldots,M, \quad (7)$$

where Υ_i is the signal-to-interference and noise ratio of the ith antenna signal, and given by

$$\Upsilon_i = \frac{\rho}{M} H_i^H \left[I + \frac{\rho}{M} \bar{H}_i \bar{H}_i^H\right]^{-1} H_i.$$

Finding a closed form solution to the above per-antenna rates seems to be a very difficult undertaking. Therefore, in addition to the analysis provided in this section, an empirical evaluation of the formula (7) is provided in subsection II.G. The empirical evaluations show that the per-antenna rates computed using (7) converge to a fixed distribution.

Moreover, in the following, we derive a lower bound on per-antenna rates by using the feedforward weights calculated based on the Zero-forcing (ZF) criterion.

D. Weights based on Zero-Forcing

When we use feedforward weights based on the Zero-forcing (ZF) criterion instead of MMSE criterion, the decoder will be suboptimal and we achieve a lower bound on the capacity. The successive decoding receiver based on the ZF criterion asymptotically achieves the channel capacity as the additive noise becomes negligible. The weight vectors of the successive decoder based on the ZF criterion are as follows:

$$B_j = H_j, \quad 1 \le j \le M-1, \quad (8)$$

$$F_k = (\bar{H}_k^T \bar{H}_k)^{-1} H_k, \quad 1 < k \le M. \quad (9)$$

The MMSE solution minimizes the squared error in the presence of channel noise, and becomes the ZF solution when no noise is present. The performance due to MMSE receivers is very similar to ZF solution when the SNR is relatively high, but is improved at low SNR's. Moreover, the true ZF solution does not always necessarily exist since the solution depends on the invertibility of $(\bar{H}_k^T \bar{H}_k)$. Assuming that the $(\bar{H}_k^T \bar{H}_k)$ is invertible, we will exploit the simplified expression of the feedforward weights in (9) to derive a closed form solution to the lower bound on the per-antenna rates.

E. Lower Bound on Per-Antenna Rates

When we use the successive decoder based on the ZF criterion instead of using MMSE, a lower bound on the ith antenna rate can be obtained:

$$R_{\{i,(M,N),ZF\}}(\rho) = E[\log_2(1+\frac{\rho}{M}\Upsilon_i)] \quad i = 1,2,\ldots,M, \quad (10)$$

where Υ_i is the signal-to-noise ratio of the ith antenna signal, and is given by

$$\Upsilon_i = H_i^H \left[\bar{H}_i \bar{H}_i^H\right]^{-1} H_i.$$

The Υ_i are independent random variables with chi-squared distribution $\Upsilon_i \sim \frac{1}{2}\chi^2_{2(N-M+i)}$. Therefore the ith antenna capacity is given by

$$R_{\{i,(M,N),ZF\}}(\rho) = E[\log_2(1+\frac{\rho}{2M}\chi^2_{2(N-M+i)})] \quad i = 1,2,\ldots,M.$$

Let $X \sim \frac{1}{2}\chi^2_{2m}$, where $m = N - M + i$. Then X has a density

$$f(x) = \frac{1}{(m-1)!} e^{-x} x^{m-1}. \quad (11)$$

Then the ith antenna rate is given by

$$R_{\{i,(M,N),ZF\}}(\rho) = \log_2 e \frac{1}{(m-1)!} \int_0^\infty dx e^{-x} x^{m-1} ln(1+\frac{\rho}{M}x). \quad (12)$$

At high signal to noise ratio, we can find an asymptotically tight close form solution to the per-antenna rate when we use the ZF based successive decoding scheme by using the fact that $\frac{\rho}{M}x >> 1$. Thus, at high SNR, the lower bound on ith antenna rate can be expressed as

$$\begin{aligned} R_{\{i,(M,N),ZF\}}(\rho) &= \frac{1}{(m-1)!} \int_0^\infty dx e^{-x} x^{m-1} ln(\frac{\rho}{M}x) \log_2 e \quad (13) \\ &= \frac{\log_2 \frac{\rho}{M}}{(m-1)!} \int_0^\infty dx e^{-x} x^{m-1} \\ &\quad + \frac{1}{(m-1)!} \int_0^\infty dx e^{-x} x^{m-1} ln(x) \log_2 e \\ &= \log_2 \frac{\rho}{M} + \left(-0.5772 + \sum_{j=1}^{m-1} \frac{1}{j}\right) \log_2 e, \end{aligned}$$

$$\Upsilon_k = \frac{\|F_k^H H_k\|^2 \frac{P}{M}}{\sum_{j=1}^{k-1} \|F_k^H (H_j - B_j)\|^2 \frac{P}{M} + \sum_{j=k+1}^{M} \|F_k^H (H_j)\|^2 \frac{P}{M} + F_k^H W F_k} \quad (3)$$

where we used the following integration formula [12]

$$\frac{1}{(m-1)!}\int_0^\infty dx e^{-x}x^{m-1}ln(x) = -0.5772 + \sum_{j=1}^{m-1}\frac{1}{j},$$

and

$$\frac{1}{(m-1)!}\int_0^\infty dx e^{-x}x^{m-1} = 1.$$

Thus, a closed form formula for lower bound on the per-antenna rate subject to the independent encoding and successive decoding algorithm in Rayleigh ergodic environment is given by

$$R_{\{i,(M,N),LB\}}(\rho) = \log_2\left[\frac{\rho}{M}\right] + \left[-0.5772 + \sum_{j=1}^{(N-M+i)-1}\frac{1}{j}\right]\log e. \quad (14)$$

F. Sum-Rates

Proposition 1: The Shannon capacity region of a MIMO channel (6) can be achieved by a combination of successive cancellation and MMSE demodulation followed by single user decoders assuming Gaussian white inputs. That is, independent antenna encoding and the optimum successive decoder and interference cancellation receiver derived from the MMSE principle is sufficient to achieve the MIMO channel capacity:

$$\begin{aligned} R_{\{(M,N),MMSE\}}(\rho) &= \sum_{i=1}^{M} C_{\{i,(M,N),MMSE\}}(\rho) \quad (15)\\ &= E\left[\log_2 \det\left(I_M + \frac{\rho}{M}H^H H\right)\right]. \end{aligned}$$

The proof of the above equation follows ([3] and [5]), which shows that the MMSE estimation process is capacity lossless.

Proposition 2: The sum capacity achieved by ZF based successive decoding scheme is strictly a lower bound on the channel capacity [10]

$$\begin{aligned} R_{\{(M,N),ZF\}}(\rho) &= \sum_{i=1}^{M} E[\log_2(1+\frac{\rho}{2M}\chi^2_{2(N-M+i)}]\\ &= \sum_{m=1}^{M}\log e\frac{1}{(m-1)!}\int_0^\infty dx e^{-x}x^{m-1}ln(1+\frac{\rho}{M}x) \quad (16)\\ &\le E\left[\log_2 \det\left(I_M + \frac{\rho}{M}H^H H\right)\right]. \end{aligned}$$

Remark 1: Note that the lower-bound for quasi-static Guassian MIMO fading channel was first derived by Foschini and Gans in [10], which is used in the proposed closed-form lower bound for the ergodic capacity of Gaussian MIMO fading channels. Moreover, recently, a tighter lower bound on the ergodic capacity is derived by Oyman et. al [11] by using multivariate statistics. However, the aim of this paper is to simultaneously find closed-form lower-bounds on the per-antenna rates, which is possible only due to (16).

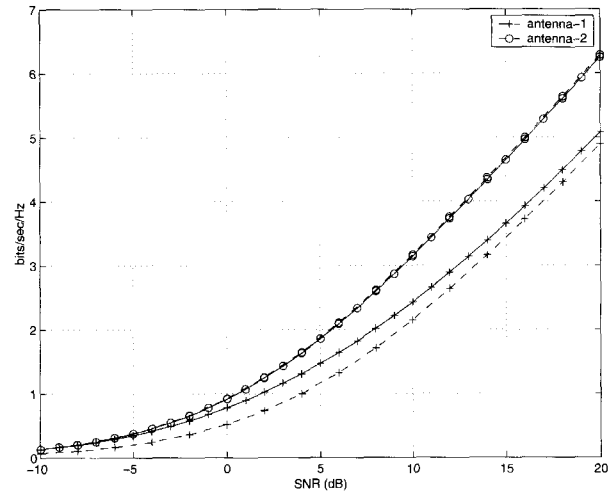

Fig. 3. Per-antenna rates vs. SNR (ρ) for 2×2 system using empirical evaluations (solid curves) and closed form lower-bound (dashed curves).

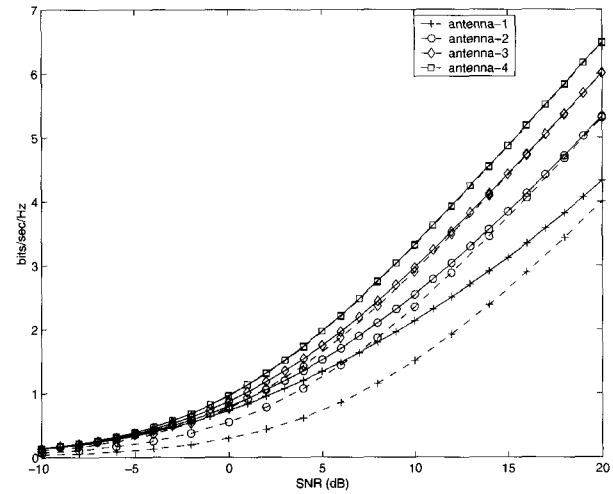

Fig. 4. Per-antenna rates vs. SNR (ρ) for 4×4 system using empirical evaluations (solid curves) and closed form lower-bound (dashed curves).

G. Numerical Results of Per-Antenna Rates

In this section, we evaluate the antenna rates using Monte-Carlo methods by integrating the rates over an iid Gaussian channel. Figs. 3-4 show the estimated antenna rates for $M = N = 2$ and 4, respectively, where the solid curves show the empirical rates (obtained using (7)) and the dashed curves show its closed form lower bound using (12). The empirical rates are estimated over 1000 independent realizations of the channel. Averaging over channel realizations was performed many times, and the capacities converged to a fixed value.

Moreover, Fig. 5 shows the sum of rates for $M = N = 2$, 4, and 8. The solid curves show the empirical capacities obtained using (6), and the dashed curves show the closed form approximation given in (16). As we can see from the figures, the closed form approximation is tight at high signal-to-noise ratios.

We are also interested in rate ratios between antennas to see the required code rate spread. Fig. 6-7 show the capacity ratio between antennas for $M = N = 2$, and 4 computed empirically.

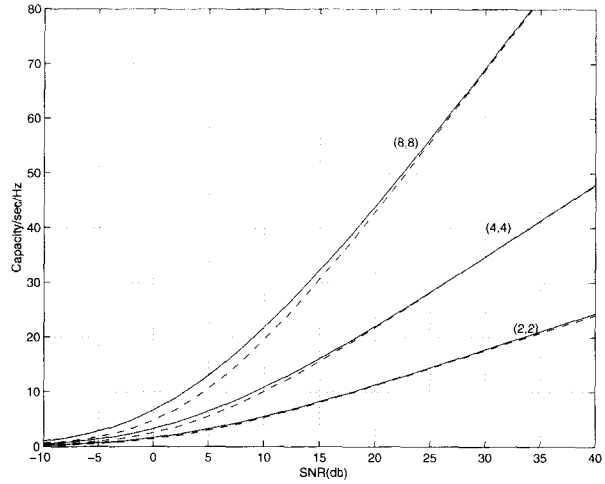

Fig. 5. Sum rates vs. SNR (ρ) for $M \times M$ system, M =2, 4, and 8 using empirical evaluations (solid curves) and closed form lower-bound (dashed curves).

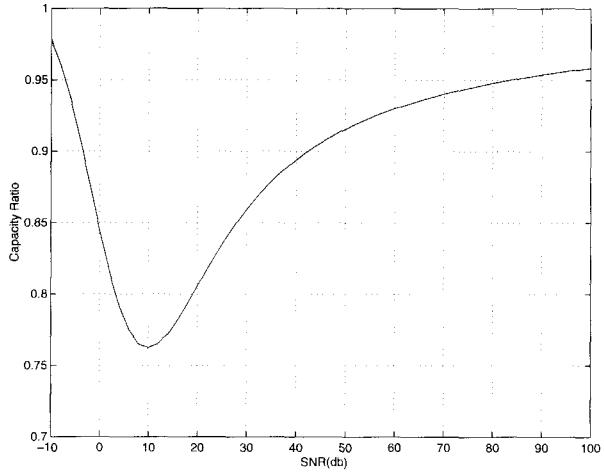

Fig. 6. Rate ratio between antenna 1 and antenna 2 vs. SNR (ρ) for a 2×2 system.

At moderate SNR, we can see a wider range of code rate spread where as at very low SNR, the code rate spread is diminishing due to the dominant receiver noise. Similarly at high SNR, due to the dominant co-antenna interference, the rate ratios converge to fixed values.

IV. MUTIRATE CODE DESIGN AND SIMULATIONS RESULTS

In this section, simulation results are presented for QPSK transmission over the ergodic MIMO channels using turbo codes with various rates. The total power P is divided equally into each antenna. That is, P/M power per antenna in a symbol interval. The performance measure is the BER under the assumption of an ideal Rayleigh channel communication scenario. We consider an ergodic channel model where the $N \times M$ matrix channel $\mathbf{H}$ changes for every symbol ("perfect interleaving" assumption) of the $M \times 1$ vector $\mathbf{a} = [a_1, a_2, \ldots, a_M]$ whose entries take on complex values in a constellation set.

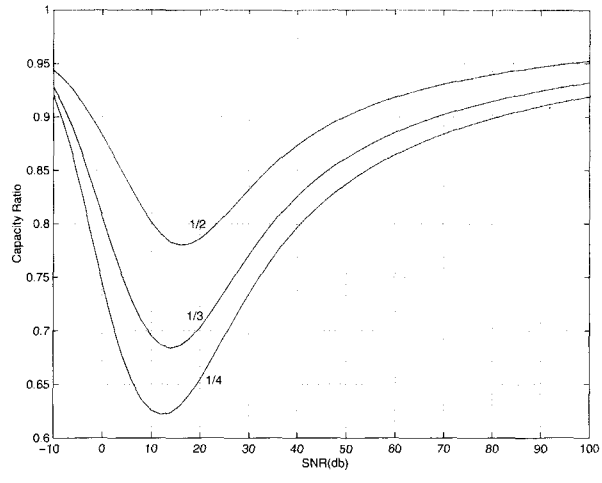

Fig. 7. Rate ratio between antenna 1 and antennas 2, 3 and 4, vs. SNR (ρ) for a 4×4 system.

A. Turbo Codes with Various Rates

For all the simulations, the turbo codes are composed of two identical 8-state convolutional codes generated by using a recursive feedback generator polynomial [1011] and a feedforward polynomial [1101]. Various code rates are obtained by puncturing the coded bits of the rate 1/3 turbo codes using similar short puncturing patterns for both convolutional component codes but with the patterns randomly replaced from one component code to the other. No effort is made to optimize the pseudo-random interleavers. In all the examples, the transmission is organized in blocks of 8012 coded bits; that is, the block size of a turbo code is fixed as 8012 coded bits per antenna regardless of its rate. Thus, to achieve various coding rates, we change the number of information bits (and the interleaver size) transmitted by an antenna. The maximum number of iterations is restricted to 20. Decoding is stopped early(using fewer than 20 full iterations), if a codeword pattern re occurs for three consecutive iterations [13]. The interference cancellation step, the errors in the previously decoded symbols are propagated in the subsequent decodings.

Fig. 8-10 show the BER performance of the successive decoding algorithm for $M = N = 2, 4$, and 8 systems. In the figures, we show the performances of two different schemes: (1) a multirate coding scheme in which each antenna is coded with a turbo code with a rate just less than its mutual information calculated according to its decoding order assuming that the operating SNR = 1.5 dB is known to the transmitter, which are shown using solid curves, and (2) equal rate turbo codes, regardless of the decoding order of the receiver, which are shown using dashed curves. In both cases, we show the BER curve for each antenna separately. As we can see from the figures, close to the receiver operating SNR =1.5 dB (please see Remark 2.2 for details), the multirate turbo coded MIMO system provides nearly an equal error protection whereas the equal rate coded systems do not. In Fig. 9, we also show the average BER performance averaged over the performances of all the transmit antennas for cases $M = N = 2$, 4, and 8, respectively (shown by the corresponding thick curves). We can see that the multirate coded scheme is able to operate with 2dB lower SNR than the

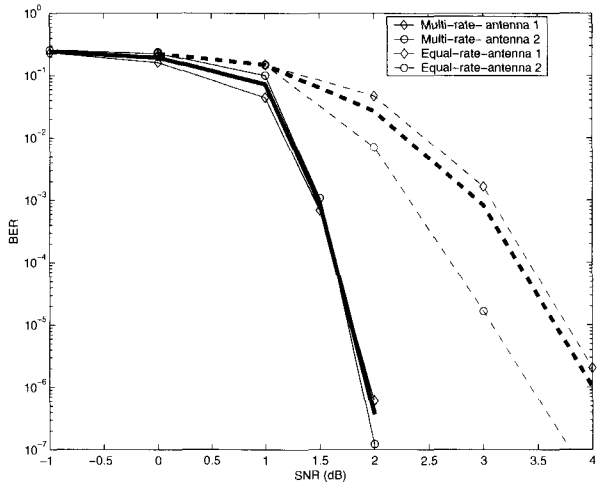

Fig. 8. BER vs. SNR (ρ) performance for 2×2 system with 8-state turbo codes. Dashed curves: Performance when rate 0.45 rate codes are used in all four antennas; Solid curves: Performance when near-optimal code rates are used in antennas 1-2, respectively. The corresponding thick curves show average BER averaged over the performances of all four antennas.

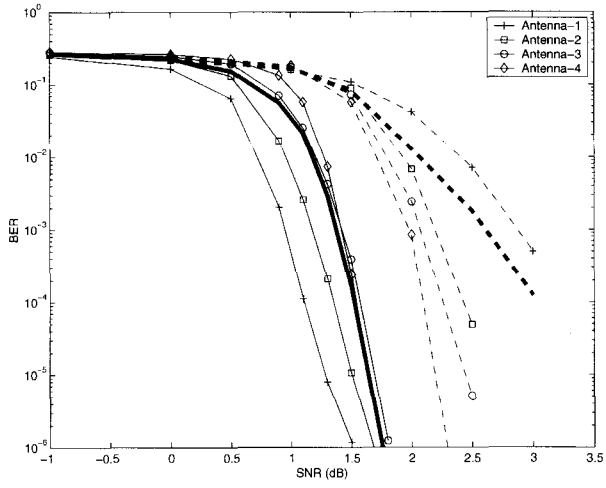

Fig. 9. BER vs. SNR (ρ) performance for 4×4 system with 8-state turbo codes. Dashed curves: Performance when rate 0.4 rate codes are used in all four antennas; Solid curves: Performance when near-optimal code rates (1/3, 0.375, 0.425, 1/2) are used in antennas 1-4, respectively. The corresponding thick curves show average BER averaged over the performances of all four antennas.

equal rate scheme at the same BER level of 10^{-5}. The multi-rate coded schemes operate very close (within 1-2 dB) to their respective capacity limits at 10^{-5} BER, Table 1. In the simulation results presented in this paper, we used (7) to calculate the antenna rates for the given channel statistics. The closed-form solution for the lower bound on the antenna rates given in (12) also can be used to calculate antenna rates to achieve near optimal performances. The performance degradation compared to the channel capacity limits are because of the performance limitation of the finite length codewords. Subsequently, any errors in the previously decoded substream will also cause errors in the subsequent decoding stages. Equation (6) is used to calculate the ideal SNR needed to achieve the specific information rate and column 5 of Table 1 lists the distance between the ideal SNR to achieve the given rates and the operating SNR.

Remark 2: 1. When we use equal rate and power allocation to every transmit antennas, the error performance is limited by the first decoded antenna (with the largest interference), where the detection/decoding order that minimizes the error performance (known as ordered serial interference cancellation (OSIC) detection and decoding) can be used in quasi-static fading situations to achieve the best possible performance. However, in ergodic channel environments, when we use channel coding across a larger block, no such ordering gain can be achieved due to the channel averaging.

2. Although, the theoretical rates of each of the antenna can be calculated to achieve the near-optimal performances given the knowledge of receiver operating SNR, due to the practical coding/decoding performance losses, the practical rates of each of the transmit antenna must be sufficiently low. For example, for the (8,8) case, empirically estimated rates at SNR =1.5 dB is [0.4532 0.4893 0.5079 0.5401 0.5817 0.6085 0.6334 0.6636], and we denoted the following slightly lower rates for actual coding: [0.334, 0.35, 0.375, 0.39, 0.40 0.425, 0.45, 0.5]. In the case of (4,4), empirically estimated rates at SNR =1.5 dB is [0.4447 0.4954 0.5524 0.6070] and the chosen rates for coding

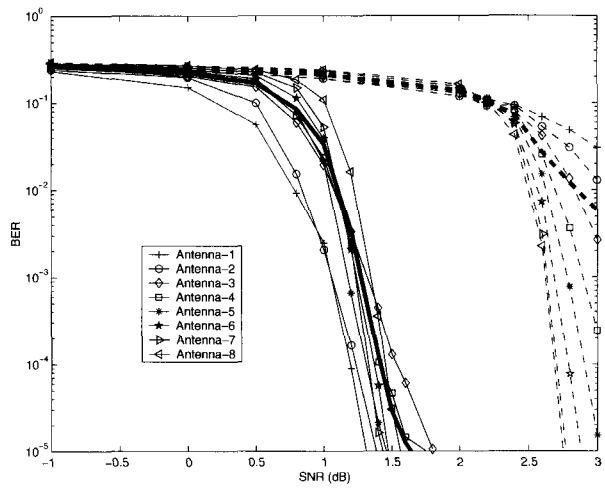

Fig. 10. BER vs. SNR (ρ) performance for 8×8 system with 8-state turbo codes. Dashed curves: Performance when rate 0.4 rate codes are used in all eight antennas; Solid curves: Performance when near-optimal code rates (1/3, 0.35, 0.375, 0.4, 0.425, 0.45, 1/2) are used in antennas 1-8, respectively. The corresponding thick curves show average BER averaged over the performances of all eight antennas.

is: [0.334, 0.375, 0.425, 0.5]. In the case of (2,2), we chose rates [0.4, 0.5] for [0.4719 0.5688] estimated at SNR=1.5dB. Moreover, the BER curves shown in Figures 8-10 are generated for the rates chosen at the operating SNR=1.5 dB. In typical environments, the receiver operating SNR must be tracked by the transmitter to adapt the transmit antenna rates.

B. Results with Known Interference

In order to confirm the proper design of the multirate coded scheme, we have also calculated the BER for the individual antennas without any error propagation in the subsequent decoding. In this comparison, instead of using the previously decoded symbols to cancel the interferences, we use the knowledge of the original transmitted symbols to cancel the interferences. Fig. 11

Table 1. Code rates used.

MIMO Configuration	Code rates	Average information rate	Operating SNR	distance to capacity limits
(2,2)	0.4, 0.5	1.9	1.5 dB	0.7 dB
(2,2)	0.45, 0.45	1.9	3.5 dB	2.8 dB
(4,4)	0.334, 0.375, 0.425, 0.5	3.26	1.5 dB	1.6 dB
(4,4)	0.4, 0.4, 0.4, 0.4	3.2	3.5 dB	3.6 dB
(8,8)	[0.334, 0.35, 0.375, 0.39, 0.40 0.425, 0.45, 0.5]	6.44	1.5 dB	1.6 dB
(8,8)	0.4, 0.4, 0.4, 0.4, 0.4, 0.4, 0.4, 0.4	6.4	4.0 dB	4.1 dB

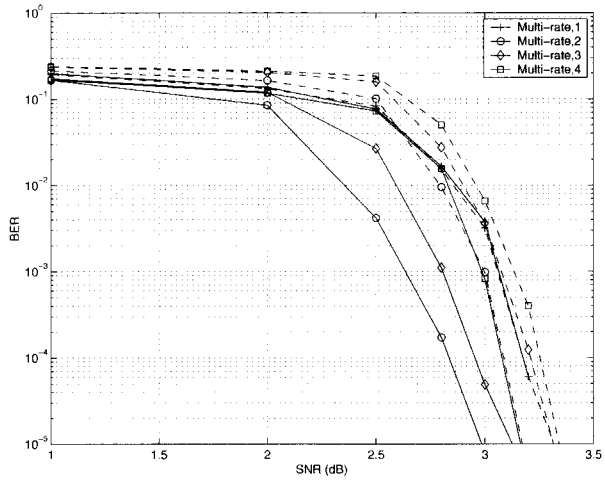

Fig. 11. BER vs. SNR (ρ) performance for 4×4 system using 8-state turbo codes with rates (0.425, 0.45, 0.52, 0.6), with known and unknown interferences. Solid curves: Performance when the exact interferences are known. Dashed curves: Performance using the decoded interferences.

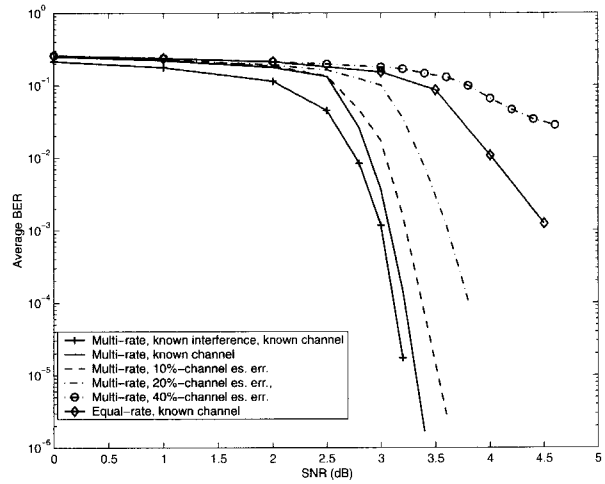

Fig. 12. Average BER vs. SNR (ρ) performance for 4×4 system using 8-state turbo codes with rates (0.425, 0.45, 0.52, 0.6), with exact and noised channel matrices.

compares the BER performances of the multirate coded system with estimated (dashed curves) and known interferences (solid curves) for $M = N = 4$ with turbo codes designed according to the antenna rates (0.425, 0.45, 0.52, 0.6) calculated for an operating SNR =3.5 dB. The curves depart from each other due to the error propagation. However, the performances of both cases (interference cancellation using known interferences and using estimated interference) are reasonably close, which shows the robustness of the turbo coded multirate system.

C. *Results with Channel Estimation Errors*

Finally, we test the the designs with channel estimation errors. For this simulation, we approximate the estimation errors by using random noise matrices such that $H_{es} = H + \Delta H$, where H is the actual channel matrix and ΔH represents the estimation error. During the detection process, the exact channel matrices were degraded by adding randomly generated complex noise matrices with normally distributed elements and variances equal to 10%, 20% and 40% of the channel power. Fig. 12 compares the average BER performances when we used the exact channel (solid curves) and noisy channel estimates with 10%, 20%, and 40% noise shown by dashed, dashed-dot and dashed-dot-circle curves, respectively, for $M = N = 4$ with turbo codes designed according to the antenna rates (0.425, 0.45, 0.52, 0.6) calculated for operating SNR =3.5 dB. The figure also compares the average performance when the receiver knows the exact channel and interferences from the previous antennas. The performances show the increasing sensitivity to the increasing channel estimation noise. Note that, to illustrate the robustness of the proposed scheme with channel estimation errors, each BER curve is generated using fixed channel estimation error variance for the chosen SNR range. However, in practice, the channel estimation error will be reduced as the SNR increases because when the receiver operates at sufficiently high SNR, the channel can be estimated more accurately. Thus, depending on the expected channel estimation errors, the per-antenna rates must be relaxed to achieve the desired BER.

V. DISCUSSIONS

We have examined the successive decoding and interference cancellation algorithm in MIMO ergodic channel environments. In particular, we have shown that rates of each antenna can be calculated using only the channel statistics so that the coding rates for each antenna are known at the transmitter. Moreover, punctured turbo codes are used to design codes with various rates for the successive decoding technique to achieve results near channel capacities.

REFERENCES

[1] A. D. Wyner, "Recent results in the Shannon theory," *IEEE Trans. Inform. Theory*, vol. IT-20, Jan. 1974.

[2] T. M. Cover, "Some advances in broadcast channels," *Advances in Communications Systems*, New York: Academic, 1975, pp. 229–260.

[3] M. K. Varanasi and T. Guess, "Optimum decision feedback multiuser equalization with successive decoding achieves the total capacity of the Gaus-

sian multiple-access channel," *Proc. Asilomar Conf. of Signal, Systems and Computers*, Monterey, CA, Nov. 1997, pp. 1405–1409.
[4] G. J. Foschini *et al.*, "Analysis and performance of some basic space-time architectures," *IEEE J. Select. Areas Commun.*, Vol. 21–3, pp. 303–320, Apr. 2003.
[5] S. L. Ariyavisitakul, "Turbo space-time processing to improve wireless channel capacity," *IEEE Trans. Commun.*, Vol. 48, No. 8, pp. 1347–1359, Aug. 2000.
[6] S. T. Chung, A. Lozano, and H. C. Huang, "Approaching eigenmode BLAST channel capacity using V-BLAST with rate and power feedback," *Proc. IEEE VTC'2001*, Fall, Atlantic city NJ, Oct. 2001.
[7] G. J. Foschini *et al.*, "Simplified processing for high spectral efficiency wireless communications employing multi-element arrays," *IEEE J. Select. Areas Commun.*, Vol. 17, No. 11, pp. 1841–1852, Nov. 1999.
[8] E. Teletar, "Capacity of multi-antenna Gaussian channels," *Technical Report., AT &T Bell Laboratories*, Murray Hill, NJ,1996.
[9] G. J. Foschini, "Layered space-time architecture for wireless communication in a fading environment when using multi-element antennas," *Bell Labs Technical Journal*, Vol. 1, No. 2, pp. 41–59, Aug. 1996.
[10] J. G. Foschini and M. J. Gans, "On limits of wireless communications in a fading environment when using multiple antennas," *Wireless Personal Communications*, 6: pp. 311–335, 1999.
[11] O. Oyman *et al.*, "Tight lower bound on the ergodic capacity of Raleigh fading MIMI channels," *Proc. IEEE Globecom'2002*, vol. 2, 2002, pp. 1172–1176.
[12] G. Ryzhik and A. Jeffrey, *Table of integrals, series, and products (5th Ed.)*, Academic Press, 1994.
[13] K. Gracie, S. Crozier, and A. Hunt, " Performance of a low-complexity turbo decoder with a simple stopping criterion implemented on a SHARC processor," *Proc. 6th IMSC'99*, Ottawa, Ontario, Canada, June 16–18, 1999, pp. 281–286.

Mathini Sellathurai received the Ph.D. degree in electrical engineering from the McMaster University, Hamilton, Canada, in 2001, and the Technical Licentiate degree in electrical engineering from the Royal Institute of Technology, Stockholm, Sweden, in 1997. She is currently a member of the Communications Signal Processing Research group in the Satellite Communications and Radio Propagation Branch, Communications Research Centre of Canada in Ottawa. Her current research interests include the applications of adaptive digital signal processing and iterative ("turbo") processing techniques to wireless communications. Dr. Sellathurai won the Natural Sciences and Engineering Research Council (NSERC) of Canada's doctoral award in the engineering and computer sciences category for her Ph.D. dissertation.

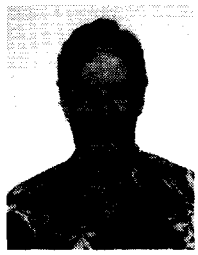

John Lodge received the B.Sc. and Ph.D. degrees in electrical engineering from Queen's University, Kingston, Ontario, in 1977 and 1981, respectively. From September 1981 to April 1984, he was with the Advanced Systems Division of Miller Communications Systems Ltd. where he was involved in the analysis and design of HF, spread-spectrum, and satellite communications systems. Since May 1984, he has been at the Communications Research Centre (CRC) in Ottawa, Canada. He is currently the Research Program Manager of the Communications Signal Processing group in the Satellite Communications and Radio Propagation Branch. His research interests pertain to the application of digital signal processing techniques to wireless communications problems, including data detection techniques in the presence of fading and the use of iterative ("turbo") processing for decoding and detection. He was the recipient of IEEE Canada's Outstanding Engineer Award in 1999, and co-recipient of the IEEE Vehicular Technology Society 1999 Neal Shepherd Best Propagation Paper Award.

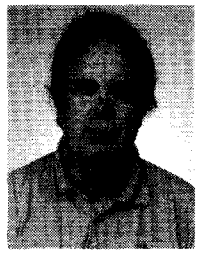

Paul Guinand received his Bachelors and Masters degrees from Queen's University, Kingston, Canada and his Ph.D. from the University of Toronto, all in mathematics. Since 1994 he has been employed by the Communications Research Centre Canada where he is a member of the Research Communications Signal Processing group.